ELSEVIER

Thermochimica Acta 253 (1995) 1–9

thermochimica acta

High temperature heat capacities of $(U_{0.91}M_{0.09})O_2$ (where M is Pr, Ce, Zr) from 290 to 1410 K ☆

Yuji Arita, Tsuneo Matsui *, Seiichi Hamada

Department of Nuclear Engineering, Faculty of Engineering, Nagoya University, Furo-cho, Chikusa-ku, Nagoya 464-01, Japan

Received 15 June 1994; accepted 15 June 1994

Abstract

Heat capacities of $(U_{0.91}M_{0.09})O_2$, where M is Pr, Ce and Zr, were measured by direct heating pulse calorimetry over the temperature range 290–1410 K. No anomalous increase in the heat capacity curve of each sample was observed at temperatures up to 1410 K, dissimilarly to the cases of $(U_{1-y}M_y)O_2$ (M is a trivalent cation (Gd, Eu, La) or simulated fission product composed of several tri- and tetravalent cations; $y = 0.044–0.142$) found previously by the present authors. It is proposed that the occurrence of the heat capacity anomaly of $(U,M)O_2$, where M is a trivalent cation or simulated fission product, originates from the predominant contribution of Frenkel pair-like defects of oxygen formed by the introduction of aliovalent cations (M^{3+}) in UO_2 from the electroneutrality condition, and that the introduction of the tetravalent cations which are the same valency as uranium ions in UO_2 results in insignificant effect on the total number of the oxygen defect, producing no heat capacity anomaly. The difference in the onset temperatures of the heat capacity anomaly of UO_2 doped with various trivalent cations is discussed from the viewpoint of the difference between the averaged cation–oxygen interatomic distance calculated from the ionic radii and that obtained from the experimental lattice constants on the assumption of the perfect fluorite structure, reflecting the variety of the distribution of oxygen around cations in the lattice, i.e. that of the local structural environments for cation–oxygen bonding. A linear relation between the onset temperature of the heat capacity anomaly and the difference in the

* Corresponding author.

☆ Presented at the International and III Sino–Japanese Symposium on Thermal Measurements, Xi'an, 4–6 June 1994.

SSDI 0040-6031(94)02020-5

cation–oxygen interatomic distance was found, supporting the importance of the variety of local structures in UO_2 as the origin of the heat capacity anomaly.

Keywords: Doping; Frenkel defects of oxygen; Heat capacity; Heat capacity anomaly

1. Introduction

The heat capacities of $(U_{1-y}M_y)O_2$, where M is Gd [1], La [2], Eu [3] and simulated fission products [4,5], have been measured over the temperature range 300–1500 K by the present authors. An anomalous increase in the heat capacity curve of each doped UO_2 sample was observed at temperatures from about 550 to 1300 K depending on the type of dopant and its concentration. This anomalous increase was interpreted as being due to the formation of Frenkel pair-like defects of oxygen [1–5], similarly to the case of UO_2 [6–8]. However there have been no data on the heat capacities of UO_2 doped with a tetravalent cation that is in the same valence state as a uranium ion in UO_2.

In the present study, the heat capacities of UO_2 doped with praseodymium, cerium and zirconium, which are thought to behave predominantly as the tetravalent cations in UO_2, were measured from 290 to 1410 K by means of direct heating pulse calorimetry to investigate the origin of the heat capacity anomaly of doped UO_2, and also to discuss the relation between the onset temperature of the heat capacity anomaly and the local structural arrangements of oxygen around dopants in UO_2.

2. Experimental

The mixture of UO_2 and MO_2 (Ce or Zr) or Pr_6O_{11}, all of which are 99.99% pure, was shaped into a cylindrical rod about 8 mm in diameter and about 40 mm in length, using an evacuated rubber press with a hydrostatic pressure of about 400 MPa. The cylindrical rod, thus prepared, was homogenized and sintered at 1573 K for 7 days in a purified argon gas flow and then at 1273 K for one day in a hydrogen gas flow in order to obtain the stoichiometric composition of oxygen ($O/(M+U) = 2.00$) according to thermogravimetric studies [9–11]. These homogenizing and sintering processes were repeated several times. X-ray analysis indicated the presence of a single fluorite phase from each sample.

The heat capacity was measured by a direct heating pulse calorimeter, details of which have been given elsewhere [12]. In this calorimeter, the temperature of a sample rod was at first increased up to the desired temperature by a platinum external heater, and after getting a constant equilibrium temperature, a current pulse was simultaneously supplied to both the sample rod and the double cylindrical molybdenum thermal shields in order to obtain the same small temperature rise (i.e. to attain the adiabatic condition). The electric potential drop, the current and

the temperature rise of the sample rod were measured to obtain the heat capacity. The heat capacity measurement was conducted within an error of ±2%, which was estimated by comparing the heat capacity of undoped UO_2 determined in this study with the previous literature values [4,13].

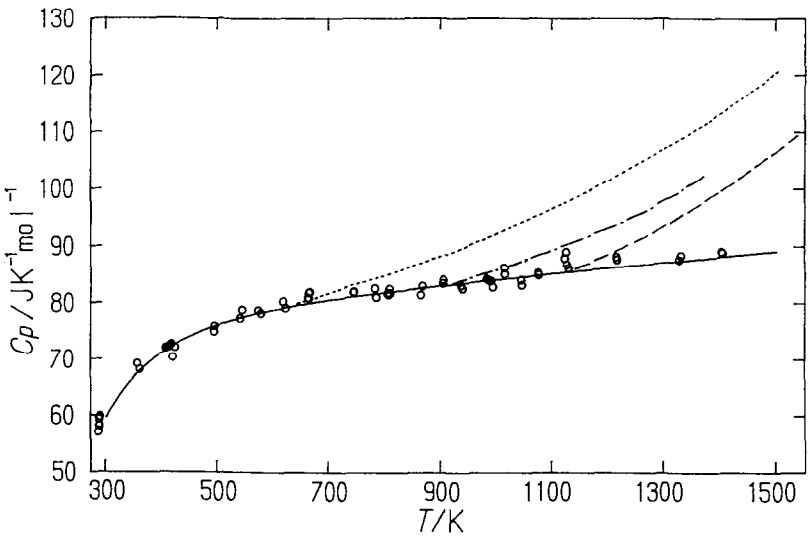

Fig. 1. Heat capacity of $(U_{0.91}Pr_{0.09})O_2$: ○, $(U_{0.91}Pr_{0.09})O_2$, this study ; ——, undoped UO_2 [1,4]; –·–, $(U_{0.899}Gd_{0.101})O_2$ [1]; – – –, $(U_{0.91}La_{0.09})O_2$ [2]; · · · ·, $(U_{0.91}FP_{0.09})O_2$ [4].

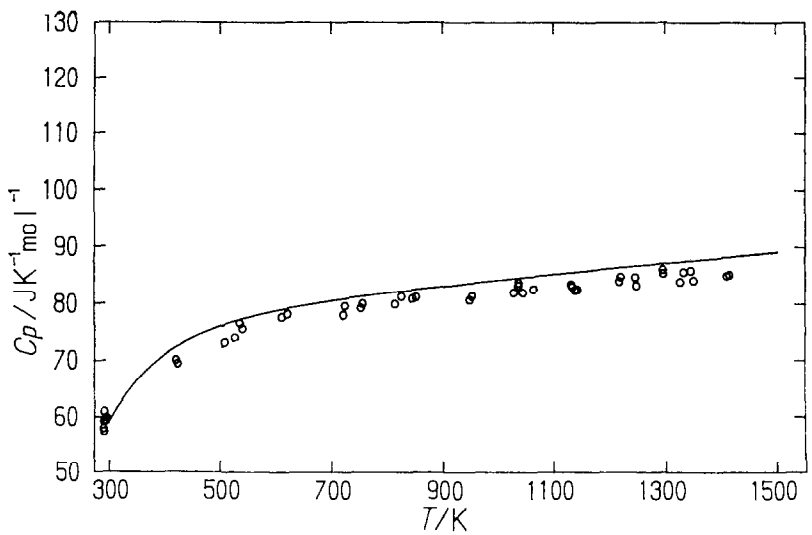

Fig. 2. Heat capacity of $(U_{0.91}Ce_{0.09})O_2$: ○, $(U_{0.91}Ce_{0.09})O_2$, this study; ——, undoped UO_2 [1,4].

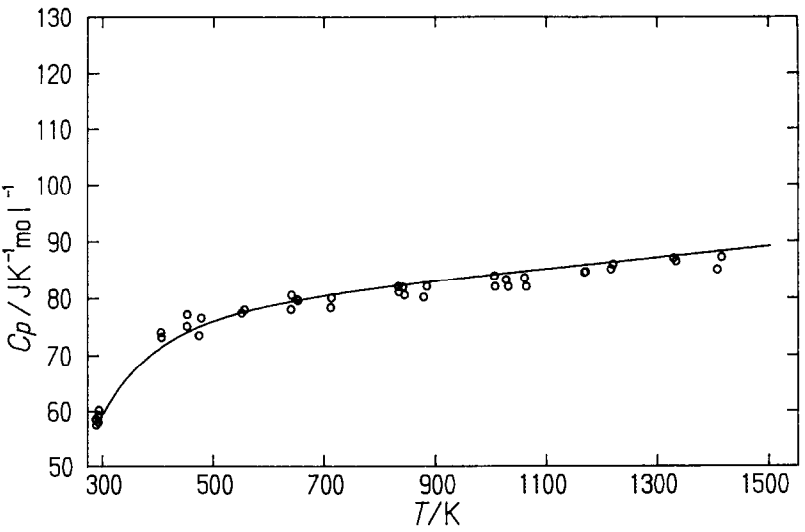

Fig. 3. Heat capacity of $(U_{0.91}Zr_{0.09})O_2$: ○, $(U_{0.91}Zr_{0.09})O_2$, this study; ——, undoped UO_2 [1,4].

3. Results and discussion

The heat capacities of UO_2 doped with 9 at% praseodymium, cerium and zirconium measured in this study are shown in Figs. 1, 2 and 3, respectively, together with the reference data of undoped UO_2 [1,4] and UO_2 doped with gadolinium [1], lanthanum [2] and simulated fission products (FP) composed of several trivalent and tetravalent cations such as yttrium, neodymium, praseodymium, cerium and zirconium [4]. As seen in these figures, no anomalous increase in the heat capacity curve of each sample is observed at temperatures up to 1410 K, dissimilarly to those of UO_2 doped with gadolinium, lanthanum and simulated fission products. The occurrence of the heat capacity anomaly of $(U,M)O_2$, where M is in the trivalent state (M^{3+}) different from the valence state of uranium ions in UO_2, has been reported to originate from the predominant contribution of Frenkel pair-like defects of oxygen formed by the introduction of aliovalent cations in UO_2 from the electroneutrality condition [1–5]. Therefore the introduction of praseodymium, cerium and zirconium ions to UO_2, which are thought to exist predominantly as the tetravalent state in UO_2, may be considered to have an insignificant effect on the total number of oxygen defects and thus no heat capacity anomaly was observed in this study.

In the figures, the temperature dependences of the heat capacities of UO_2 doped with praseodymium, cerium and zirconium are also seen to be similar to that of undoped UO_2. The respective equations for the heat capacity curves of $(U_{0.91}Pr_{0.09})O_2$, $(U_{0.91}Ce_{0.09})O_2$ and $(U_{0.91}Zr_{0.09})O_2$ are determined by the least-squares method as

$$C_p/(\mathrm{J\ K^{-1}\ mol^{-1}}) = 80.185 + 6.5829 \times 10^{-3}(T/\mathrm{K}) - 1.8930 \times 10^{6}(T/\mathrm{K})^{-2} \quad (1)$$

where $285 \leqslant T/\mathrm{K} \leqslant 1412$.

$$C_p/(\mathrm{J\ K^{-1}\ mol^{-1}}) = 75.498 + 7.5109 \times 10^{-3}(T/\mathrm{K}) - 1.5883 \times 10^{6}(T/\mathrm{K})^{-2} \quad (2)$$

where $286 \leqslant T/\mathrm{K} \leqslant 1413$.

$$C_p/(\mathrm{J\ K^{-1}\ mol^{-1}}) = 82.498 + 2.9201 \times 10^{-3}(T/\mathrm{K}) - 1.9969 \times 10^{6}(T/\mathrm{K})^{-2} \quad (3)$$

where $285 \leqslant T/\mathrm{K} \leqslant 1412$.

The difference in the onset temperatures of the anomalous increase in the heat capacity curves of UO_2 doped with various cations was previously discussed by the author and co-workers [3–5,14] in relation to the change of the lattice constant per

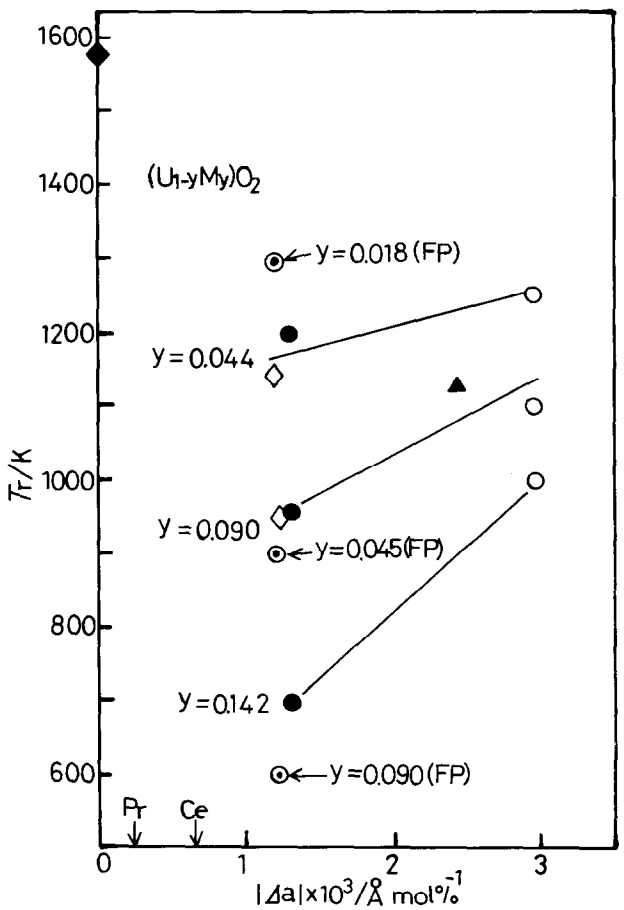

Fig. 4. Relation between the onset temperature of the heat capacity anomaly and the change in the lattice constant of doped UO_2 per mol% of dopant: ●, Gd [1]; ○, La [2]; ◇, Eu [3]; △, Y [4]; ⊙, FP [4,5]; ◆, undoped UO_2 estimated in Ref. [14].

mol% of dopant ($|\Delta a|$) in UO_2 calculated from the experimental lattice constants of doped UO_2 and undoped UO_2. In Fig. 4, where the onset temperatures (T_r) are plotted against $|\Delta a|$, the onset temperatures of $(U_{1-y}M_y)O_2$ with constant dopant concentration y except for $(U_{1-y}FP_y)O_2$ increase linearly with increasing $|\Delta a|$, indicating the smaller elastic strain renders the onset temperature lower. The fact that the ionic conductivity of doped fluorite-type oxides such as ZrO_2 doped with trivalent cations, where the oxygen ion is the predominant mobile species, decreases with increasing $|\Delta a|$ as reviewed by Kim [15], also supports the dependence of the onset temperature upon the $|\Delta a|$ value, because the Frenkel pair-like defect of oxygen can be formed more easily under the conditions that make oxygen ion more mobile. The onset temperatures of $(U_{1-y}FP_y)O_2$ previously reported [4,5], however, are seen to be apart from the straight line drawn using the onset temperatures of UO_2 doped with a single cation, $(U_{1-y}M_y)O_2$. Moreover, no heat capacity anomaly is seen in these studies up to 1410 K in UO_2 doped with praseodymium and cerium, as shown in Figs. 1 and 2, respectively, differently from the low onset temperatures expected from small $|\Delta a|$ of UO_2 doped with praseodymium and cerium as marked in the abscissa in Fig. 4.

The local structural environments of Y^{3+} and Zr^{4+} ions in 18 wt% Y_2O_3 doped ZrO_2 were studied using extended X-ray absorption fine structure spectroscopy (EXAFS) over the temperature range 153–1043 K [16]. The oxygen arrangements around Y^{3+} and Zr^{4+} were found to be different, i.e. more oxygen vacancies were sited adjacent to Zr^{4+} and were more disordered than Y^{3+} at low temperature. The structural environment of Zr^{4+} in cubic ZrO_2 resembled that of the seven-coordinated Zr^{4+} in monoclinic ZrO_2. Increasing the temperature of the sample resulted in the local structural environments of two cations becoming more alike, suggesting that increased oxygen mobility leads to an increasing random distribution of oxygen defects. Therefore, similarly to the case of ZrO_2, the oxygen arrangement around M^{3+} dopants in UO_2, which has the same fluorite structure as ZrO_2, is thought to be different from that around uranium ions. It is also expected that, with increasing temperature, oxygen mobility is increased such as to make the distribution of oxygen defects around M^{3+} and U^{4+} average (disorder), resulting in the heat capacity anomaly.

In the present paper, the variety of the oxygen arrangement around cations in UO_2 is assumed to be related to the value of ΔX expressed by Eq. (4), i.e. the difference between the averaged cation–oxygen interatomic distance obtained from the ionic radii in Shannon's table [17] and that calculated from the experimental lattice constants of doped UO_2 based on the perfect fluorite structure

$$\Delta X = [(r_c + r_o) - \sqrt{3}/4a_1]_A - [(r_u + r_o) - \sqrt{3}/4a_2]_B \quad (4)$$

where A and B represent the values in doped UO_2 and undoped UO_2, respectively. The values of r_c, r_o and r_u, which are, respectively, the average ionic radius of all cations (M^{3+}, U^{4+}, U^{5+}) with eightfold coordination in doped UO_2, the ionic radius of an oxygen ion with fourfold coordination and the ionic radius of a uranium ion with eightfold coordination, were taken from those reported by Shannon [17]. The values of the lattice constants of doped UO_2 (a_1) and undoped

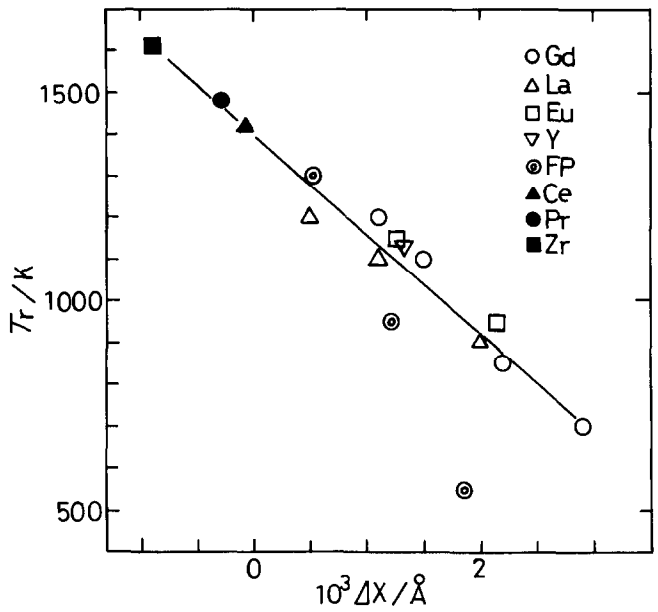

Fig. 5. Relation between the onset temperature of the heat capacity anomaly and the value of ΔX given by Eq. (4) for UO_2 doped with trivalent ions of Gd, La, Eu and Y, the tetravalent ions of Ce, Pr and Zr, and the simulated fission products composed of the trivalent Nd and Y, and tetravalent Ce, Pr and Zr ions.

UO_2 (a_2) were given experimentally [11,17–22]. In Fig. 5 the onset temperatures (T_r) of the heat capacity anomaly of $(U_{1-y}M_y)O_2$ (where M is Y, Gd, La, Eu and FP; $y = 0.018$–0.142) are plotted against ΔX. It is seen in this figure that the onset temperatures of doped UO_2, regardless of the type and the concentrations y of dopants, except for $(U_{1-y}FP_y)O_2$, decrease linearly with increasing ΔX along one line, indicating the larger change in the average cation–oxygen interatomic distance (i.e. the more complicated distribution of oxygen defects) caused by the introduction of aliovalent cation renders the onset temperature lower. The onset temperatures of $(U_{1-y}FP_y)O_2$ are seen to deviate from the line with increasing ΔX (i.e. y value). Because the value of ΔX for $(U_{1-y}FP_y)O_2$ was calculated by Eq. (4) with the averaged cation radius of all the many cations (Nd^{3+}, Y^{3+}, Ce^{4+}, Pr^{4+}, Zr^{4+}, U^{4+}, U^{5+}) assuming the applicability of the same procedure as for UO_2 doped with a single cation, the variety (complexity) of the local structures of oxygens (or degree of disordering of the oxygen arrangement) around cations is not thought to be suitably expressed by the ΔX value alone. It is also noted in Fig. 5 that the onset temperatures of UO_2 doped with Pr^{4+}, Ce^{4+} and Zr^{4+} are given on the assumption of the presence of the heat capacity anomaly and of the same linear relation between ΔX and T_r applying. The assumed onset temperatures of UO_2 doped with tetravalent praseodymium, cerium and zirconium ions, thus estimated, are higher

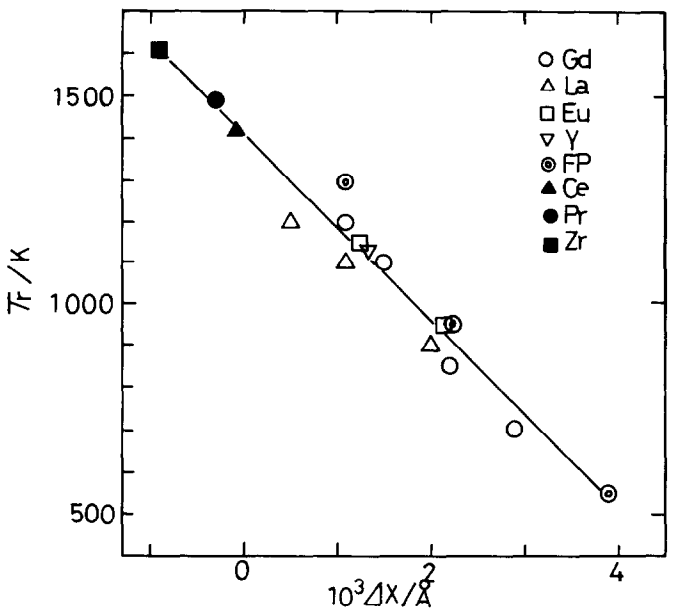

Fig. 6. Relation between the onset temperature of the heat capacity anomaly and the value of ΔX for UO_2 doped with the trivalent ions, tetravalent ions, and the simulated fission products that are assumed to be composed of all trivalent Nd, Y, Ce, Pr and Zr ions.

than 1420 K which is above the upper temperature limit of the present heat capacity measurements. It is, therefore, not clear at present whether the heat capacity anomaly in UO_2 doped with these tetravalent cations exists. In Fig. 6 the onset temperatures of the heat capacity anomaly of $(U_{1-y}FP_y)O_2$ ($y = 0.018$, 0.045 and 0.090) are plotted against modified ΔX values obtained from Eq. (4) assuming that all constituent cations (Nd, Y, Ce, Pr and Zr) in the simulated fission products are present in the trivalent state in UO_2, so reflecting, to a first approximation, the complexity of the presence of many different local structures of oxygen around cations upon Eq. (4); the bigger ionic radius of trivalent cations compared to tetravalent cations produces larger ΔX values, i.e. a greater complexity of oxygen arrangements, inducing the easy formation of oxygen defects for the heat capacity anomaly. The values of T_r, thus plotted, are seen to be close to a line drawn for the data of $(U_{1-y}M_y)O_2$. To make clear the validity of the present discussion, the precise structural analysis by EXAFS is now in progress in our laboratory.

4. Conclusions

(1) No anomalous increase in the heat capacity curves of $(U_{0.91}M_{0.09})O_2$ (where M is Pr, Ce, Zr) was seen over the temperature range up to 1410 K dissimilarly to

the cases of $(U_{1-y}M_y)O_2$ (where M is trivalent cations Gd, Eu, La, Y and simulated fission products) found previously by the author and co-workers.

(2) The occurrence of the heat capacity anomaly of doped UO_2 is thought to originate from the predominant contribution of oxygen defects formed by the introduction of aliovalent (trivalent) cations in UO_2 from the electroneutrality condition. Therefore, the introduction of the tetravalent cations (Pr, Ce, Zr) in the present study results in an insignificant effect on the total number of oxygen defects, producing no heat capacity anomaly.

(3) The onset temperatures of the heat capacity anomaly observed for UO_2 doped with trivalent cations decreased with increasing ΔX, the difference between the averaged cation–oxygen interatomic distance obtained from the ionic radii and that calculated from the experimental lattice constants. Because the difference ΔX, thus obtained, is thought to be related to the degree of the complexity of the distribution of oxygen defects around cations in the UO_2 lattice, i.e. the complexity of the local structural environments for cation–oxygen bonding, the larger difference induces easy formation of oxygen defects and thus decreases the onset temperature of the heat capacity anomaly.

References

[1] H. Inaba, K. Naito and M. Oguma, J. Nucl. Mater., 149 (1987) 341.
[2] T. Matsui, Y. Arita and K. Naito, J. Radioanal. Nucl. Chem., 143 (1991) 149.
[3] T. Matsui, T. Kawase and K. Naito, J. Nucl. Mater., 186 (1992) 254.
[4] T. Matsui, Y. Arita and K. Naito, J. Nucl. Mater., 188 (1992) 205.
[5] Y. Arita, S. Hamada and T. Matsui, Thermochim. Acta, in press.
[6] J.F. Kerrisk and D.G. Clifton, Nucl. Technol., 16 (1972) 531.
[7] R. Szwarc, J. Phys. Chem. Solids, 30 (1969) 705.
[8] P. Browning, J. Nucl. Mater., 98 (1981) 345.
[9] T.L. Markin and E.C. Crough, J. Inorg. Nucl. Chem., 32 (1970) 77.
[10] T. Yamashita and T. Fujino, Paper presented at the Annual Meeting of the Japan Atomic Energy Society, Tokyo, Japan, 1989, J3.
[11] S. Aronson and J.C. Clayton, J. Chem. Phys., 35 (1961) 1055.
[12] K. Naito, H. Inaba, M. Ishida and K. Seta, J. Phys. E, 12 (1979) 712.
[13] F. Grønvold, N.J. Kveseth, A. Sveen and J. Tichy, J. Chem. Thermodyn., 2 (1970) 665.
[14] T. Matsui and K. Naito, J. Nucl. Mater., 138 (1989) 19.
[15] D.J. Kim, J. Am. Ceram. Soc., 72 (1989) 1415.
[16] C.R.A. Catlow, A.V. Chadwick, G.N. Greaves and L.M. Moroney, J. Am. Ceram. Soc., 69 (1986) 272.
[17] R.D. Shannon, Acta Crystallogr., Sect. A, 32 (1976) 751.
[18] W.A. Young, L. Lynds and J.S. Mohl, NAA-SR-6765, USA, 1962.
[19] T. Ohmichi, S. Fukushima, M. Maeda and H. Watanabe, J. Nucl. Mater., 102 (1981) 40.
[20] T. Yamashita, T. Fujino and H. Tagawa, J. Nucl. Mater., 132 (1985) 192.
[21] D.I.R. Norris and P. Kay, J. Nucl. Mater., 116 (1983) 184.
[22] K. Une and M. Oguma, J. Nucl. Sci. Technol., 20 (1983) 844.